

RESEARCH ARTICLE

terminated whether this promoted insulin resistance when injected into mice. Intraperitoneal injection of insulin (0.5 U/kg) and purified Klotho extracellular peptide (10 µg/kg, Fig. 2F) in wild-type male and female mice attenuated the hypoglycemic response expected from insulin alone (Fig. 2G). Klotho peptide alone rapidly increased blood glucose levels in male wild-type mice and to a smaller extent in females (Fig. 2H). However, Klotho peptide injection did not induce significant changes in blood insulin and glucagon levels (fig. S4), suggesting that Klotho peptide inhibits insulin action directly in peripheral tissues.

To test whether Klotho antagonizes insulin at receptive cells, we determined whether re-

combinant Klotho peptide would reduce glucose uptake by blocking insulin binding to the insulin receptor. We measured cellular glucose uptake in cultured myoblastic cells (L6) incubated with or without insulin in the presence or absence of 100 pM of Klotho extracellular peptide. Klotho peptide suppressed insulin-induced glucose uptake by 55% without reducing the binding of [¹²⁵I] insulin to the cells (fig. S5). Thus, Klotho does not appear to inhibit ligand-binding to the insulin receptor, suggesting that Klotho may block insulin action by disrupting one or more alternative insulin-dependent intracellular signaling pathways. Accordingly, we measured the potential for [¹²⁵I]-labeled Klotho to bind directly to the cell surface. Hepatoma cells

bound [¹²⁵I] Klotho in a dose-dependent manner and saturated when the total Klotho concentration exceeded 600 pM, and unlabeled Klotho peptide inhibited the binding of [¹²⁵I] Klotho (fig. S6). Together, these observations suggest that cells present a receptor at their surface other than the insulin receptor that binds to the Klotho peptide.

Klotho inhibits intracellular insulin and IGF1 signaling. Because membrane-bound Klotho peptide must inhibit ligand activation of the insulin receptor within the cells, we investigated the influence of Klotho on insulin receptor signal transduction (25, 26). We incubated L6 cells or rat hepatoma cells (H4IIE) with recombinant Klotho peptide and insulin (10 nM) or IGF1 (10 nM). Klotho peptide did not inhibit the binding of [¹²⁵I] insulin or [¹²⁵I] IGF1 (fig. S5) but suppressed ligand-stimulated autophosphorylation of insulin and IGF1 receptors in a dose-dependent manner (Fig. 3, A and B). Additionally, Klotho reduced activation of signaling events downstream of receptor activation, including tyrosine-phosphorylated insulin receptor substrate (IRS) 1 and 2, the association of the subunit of phosphoinositide 3-kinase p85 with IRS proteins (Fig. 3, A and B). Because the inhibitory effect of Klotho on insulin signaling was observed as early as 1 min after insulin stimulation (Fig. 3C), the decline in tyrosine-phosphorylated insulin and IGF1 receptors is unlikely due simply to the loss of receptors. Notably, Klotho peptide can inactivate active insulin receptors that were previously tyrosine phosphorylated by insulin stimulation. In H4IIE cells that were exposed to 10 nM insulin before adding Klotho peptide, Klotho suppressed tyrosine phosphorylation of the insulin receptor (Fig. 3D). We observed a similar effect on IGF1 receptor autophosphorylation in L6 cells with IGF1 before adding Klotho peptide (9). Importantly, the inhibitory effect of Klotho on autophosphorylation of receptor tyrosine kinases is specific. We observed no inhibitory effect of Klotho on the epidermal growth factor receptor and the platelet-derived growth factor receptor (fig. S7). Overall, Klotho appears to inhibit activation of the insulin and IGF1 receptor and to repress activated insulin and IGF1 receptors. Whether Klotho peptide functions by accelerating removal of tyrosine phosphorylation from the activated insulin receptor remains to be determined.

Inhibition of insulin and IGF1 signaling rescues *KL*^{-/-} phenotypes. If the ability of Klotho to inhibit insulin and IGF1 signaling extends survival by retarding senescence, independent manipulations to inhibit insulin and IGF1 signaling may ameliorate some of the aging-like phenotypes in *KL*^{-/-} mice. Accordingly, we crossed a loss-of-function mutation of IRS-1 into the *KL*^{-/-} mice (27). Survival was improved in *KL*^{-/-} mice heterozygous for an IRS-1 null allele (*KL*^{-/-} *IRS-1*^{+/-}) relative to *KL*^{-/-} control mice

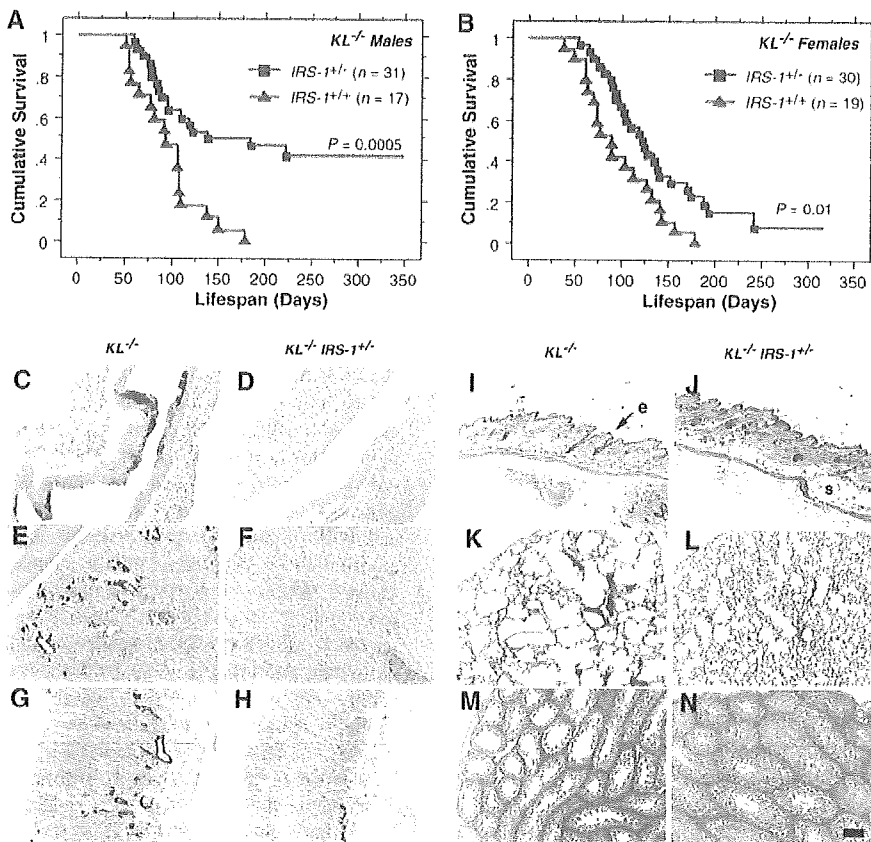


Fig. 4. Rescue of aging-like phenotypes in *KL*^{-/-} mice by genetic intervention in insulin and IGF1 signaling. (A and B) Life-span extension in *KL*^{-/-} mice by reducing IRS-1 expression. *KL*^{-/-} mice heterozygous for an IRS-1 null allele (*IRS-1*^{+/-}) lived longer than those without the mutation (*IRS-1*^{+/+}) both in males ($P = 0.0005$ by log-rank test) and females ($P = 0.01$ by log-rank test). [(C) to (N)] Rescue of aging-like phenotypes in *KL*^{-/-} *IRS-1*^{+/-} mice at the histological level. Typical findings from four 8-week-old males of each genotype are shown. (C and D) Aorta (von Kossa staining). Calcification of arterial walls [black deposits in (C)] was decreased in *KL*^{-/-} *IRS-1*^{+/-} mice (D). (E and F) Kidney (von Kossa staining). Calcification of small arteries and renal tubules [black deposits in (E)] was decreased in *KL*^{-/-} *IRS-1*^{+/-} mice (F). (G and H) Stomach (von Kossa staining). Ectopic calcification in gastric mucosa and small arteries [black deposits in (G)] was alleviated in *KL*^{-/-} *IRS-1*^{+/-} mice (H). (I and J) Cross-sections of the skin. Hematoxylin-eosin (HE) staining. Reduction in epidermal layer (e) thickness observed in *KL*^{-/-} mice (I) was improved and subcutaneous fat (s) was restored in *KL*^{-/-} *IRS-1*^{+/-} mice (J). (K and L) Lung (HE staining). Emphysematous changes, including enlargement of air spaces and destruction of the normal alveolar architecture were observed in *KL*^{-/-} mice (K), but were alleviated in *KL*^{-/-} *IRS-1*^{+/-} mice (L). (M and N) Testis (HE staining). Seminiferous tubules were atrophic and no mature sperm was observed in *KL*^{-/-} mice (M). Spermatogenesis was restored in *KL*^{-/-} *IRS-1*^{+/-} mice (N). All panels were shown in the identical magnification ($\times 200$). Scale bar, 200 µm.

(Fig. 4, A and B). In addition, $KL^{-/-} IRS-1^{+/-}$ mice ameliorated many age-related pathologies typical of $KL^{-/-}$ mice, including arteriosclerosis, ectopic calcification, skin atrophy, pulmonary emphysema, and hypogonadism (Fig. 4, C to N). Heterozygosity of $IRS-1$ alone ($KL^{+/+} IRS-1^{+/-}$ littermates) appears to have no effect on survival and the age-progressive degeneration when compared with those factors in wild-type littermates during these experiments (9).

Conclusion. We previously reported that a defect in *Klotho* gene expression leads to a syndrome that may resemble premature aging (1). Here, we show that overexpression of *Klotho* can extend life span, and we suggest that *Klotho* functions as an aging suppressor gene in mammals. We found that the extracellular domain of *Klotho* protein circulates in the blood and binds to a putative cell-surface receptor. *Klotho* has marked effects on insulin physiology, apparently because it suppresses tyrosine phosphorylation of insulin and IGF1 receptors, which results in reduced activity of IRS proteins and their association with PI3-kinase, thereby inhibiting insulin and IGF1 signaling. Extended life span upon negative regulation of insulin and IGF1 signaling is an evolutionarily conserved mechanism to suppress aging (28). *Klotho* appears to be a peptide

hormone to modulate such signaling and thereby mediate insulin metabolism and aging.

References and Notes

1. M. Kuro-o et al., *Nature* 390, 45 (1997).
2. Y. Takahashi, M. Kuro-o, F. Ishikawa, *Proc. Natl. Acad. Sci. U.S.A.* 97, 12407 (2000).
3. D. E. Arking et al., *Proc. Natl. Acad. Sci. U.S.A.* 99, 856 (2002).
4. D. E. Arking et al., *Am. J. Hum. Genet.* 72, 1154 (2003).
5. N. Ogata et al., *Bone* 31, 37 (2002).
6. K. Kawano et al., *J. Bone Miner. Res.* 17, 1744 (2002).
7. Y. Yamada, F. Ando, N. Niino, H. Shimokata, *J. Mol. Med.* 83, 50 (2005).
8. D. E. Arking, G. Atzmon, A. Arking, N. Barzilai, H. C. Dietz, *Circ. Res.* 96, 412 (2005).
9. M. Kuro-o et al., data not shown.
10. F. Grabnitz, M. Seiss, K. P. Rucknagel, W. L. Staudenbauer, *Eur. J. Biochem.* 200, 301 (1991).
11. R. Weindruch, R. L. Walford, S. Fligiel, D. Guthrie, *J. Nutr.* 116, 641 (1986).
12. H. M. Brown-Borg, K. E. Borg, C. J. Meliska, A. Bartke, *Nature* 384, 33 (1996).
13. R. A. Miller, *Sci. Aging Knowledge Environ.* 2001, vp6 (2001).
14. G. C. Williams, *Evol. Int. J. Org. Evol.* 11, 398 (1957).
15. C. Kenyon, J. Chang, E. Gensch, A. Rudner, R. Tabtiang, *Nature* 366, 461 (1993).
16. J. Z. Morris, H. A. Tissenbaum, G. Ruvkun, *Nature* 382, 536 (1996).
17. M. Tatar et al., *Science* 292, 107 (2001).
18. D. J. Clancy et al., *Science* 292, 104 (2001).
19. M. Holzenberger et al., *Nature* 421, 182 (2003).
20. M. Blüher, B. B. Kahn, C. R. Kahn, *Science* 299, 572 (2003).
21. C. Kenyon, *Cell* 120, 449 (2005).
22. T. Utsugi et al., *Metabolism* 49, 1118 (2000).
23. A. E. Halseth, D. P. Bracy, D. H. Wasserman, *Am. J. Physiol.* 276, E70 (1999).

24. A. Imura et al., *FEBS Lett.* 565, 143 (2004).
 25. A. R. Saltiel, C. R. Kahn, *Nature* 414, 799 (2001).
 26. D. LeRoith, C. T. Roberts Jr., *Cancer Lett.* 195, 127 (2003).
 27. E. Araki et al., *Nature* 372, 186 (1994).
 28. M. Tatar, A. Bartke, A. Antebi, *Science* 299, 1346 (2003).
- We thank D. H. Wasserman and Vanderbilt Mouse Metabolic Phenotyping Center for physiological analysis of the mice; R. L. Dobbins for hyperinsulinemic euglycemic clamp experiments; J. A. Richardson and Molecular Pathology Core Facility at UT Southwestern for histological analysis; D. W. Russell at UT Southwestern for Klotho receptor identification; R. Komuro and H. Kuriyama at UT Southwestern for insulin and IGF1 signaling analysis; Genentech for providing IGF1; H. Masuda, T. Suga, R. Nagai, A. T. Dang, R. Shamlou, P. Bezerra, T. Reed, C. Iucu, W. Lai for earlier contributions and supports to this study; and E. C. Friedberg, M. S. Brown, and K. A. Wharton Jr. at UT Southwestern for critical reading of the manuscript. This work was supported in part by grants from Endowed Scholar Program at UT Southwestern (M.K.), Pew Scholars Program in Biomedical Science (M.K.), Eisai Research Fund (M.K.), High-Impact/High-Risk Research Program at UT Southwestern (M.K.), and NIH (R01AG19712 to M.K. and R01AG25326 to M.K. and K.P.R.). J.H. is supported by the NIH, the Perot Family Foundation, and the Humboldt Foundation.

Supporting Online Material

www.sciencemag.org/cgi/content/full/1112766/DC1
Materials and Methods

Figs. S1 to S7

Table S1

References

25 March 2005; accepted 4 August 2005

Published online 25 August 2005;

10.1126/science.1112766

Include this information when citing this paper.

REPORTS

Bright X-ray Flares in Gamma-Ray Burst Afterglows

D. N. Burrows,^{1*} P. Romano,² A. Falcone,¹ S. Kobayashi,^{1,3} B. Zhang,⁴ A. Moretti,² P. T. O'Brien,⁵ M. R. Goad,⁵ S. Campana,² K. L. Page,⁵ L. Angelini,^{6,7} S. Barthelmy,⁶ A. P. Beardmore,⁵ M. Capalbi,⁸ G. Chincarini,^{2,9} J. Cummings,⁶ G. Cusumano,¹⁰ D. Fox,¹¹ P. Giommi,⁸ J. E. Hill,¹ J. A. Kennea,¹ H. Krimm,⁶ V. Mangano,¹⁰ F. Marshall,⁶ P. Mészáros,¹ D. C. Morris,¹ J. A. Nousek,¹ J. P. Osborne,⁵ C. Pagani,^{1,2} M. Perri,⁸ G. Tagliaferri,² A. A. Wells,⁵ S. Woosley,¹² N. Gehrels⁶

Gamma-ray burst (GRB) afterglows have provided important clues to the nature of these massive explosive events, providing direct information on the nearby environment and indirect information on the central engine that powers the burst. We report the discovery of two bright x-ray flares in GRB afterglows, including a giant flare comparable in total energy to the burst itself, each peaking minutes after the burst. These strong, rapid x-ray flares imply that the central engines of the bursts have long periods of activity, with strong internal shocks continuing for hundreds of seconds after the gamma-ray emission has ended.

Gamma-ray bursts (GRBs) are the most powerful explosions since the Big Bang, with typical energies around 10^{51} ergs. Long GRBs (duration > 2 s) are thought to signal the creation

of black holes by the collapse of massive stars (1–4). The detected signals from the resulting highly relativistic fireballs consist of prompt gamma-ray emission (from internal shocks in

the fireball) lasting for several seconds to minutes, followed by afterglow emission (from external shocks as the fireball encounters surrounding material) covering a broad range of frequencies from radio through x-rays (5–7). Because of the time needed to accurately determine the GRB position, most afterglow

- ¹Department of Astronomy and Astrophysics, 525 Davey Lab, Pennsylvania State University, University Park, PA 16802, USA. ²Istituto Nazionale di Astrofisica (INAF)—Osservatorio Astronomico di Brera, Via Bianchi 46, 23807 Merate, Italy. ³Center for Gravitational Wave Physics, 104 Davey Lab, Pennsylvania State University, University Park, PA 16802, USA. ⁴Department of Physics, University of Nevada, Box 454002, Las Vegas, NV 89154–4002, USA. ⁵Department of Physics and Astronomy, University of Leicester, University Road, Leicester LE1 7RH, UK. ⁶NASA/Goddard Space Flight Center, Greenbelt, MD 20771, USA. ⁷Department of Physics and Astronomy, Johns Hopkins University, 3400 North Charles Street, Baltimore, MD 21218, USA. ⁸Agenzia Spaziale Italiana Science Data Center, Via Galileo Galilei, 00044 Frascati, Italy. ⁹Dipartimento di Fisica, Università degli studi di Milano-Bicocca, Piazza delle Scienze 3, 20126 Milan, Italy. ¹⁰INAF—Istituto di Astrofisica Spaziale e Fisica Cosmica Sezione di Palermo, Via Ugo La Malfa 153, 90146 Palermo, Italy. ¹¹Department of Astronomy, California Institute of Technology, MS 105-24, Pasadena, CA, 91125, USA. ¹²Department of Astronomy and Astrophysics, University of California, Santa Cruz, CA 95064, USA.

*To whom correspondence should be addressed. E-mail: burrows@astro.psu.edu